Hydrogen from water electrolysis

24

Greig Chisholm, Tingting Zhao and Leroy Cronin
School of Chemistry, University of Glasgow, Glasgow, United Kingdom

1. Introduction

Renewable energy continues to show strong growth (Fig. 24.1), particularly in wind and solar PV [1].

Despite great technological advancements, it is not possible to match the predictable peaks and troughs of energy demand with the unpredictable peaks and troughs of energy supply from renewable sources. This issue necessitates the continued use of conventional and rapidly responding energy sources predominantly based on the combustion of hydrocarbon-based fuels to maintain energy supplies. As a result, this approach can lead to scenarios wherein demand is low and is being met by conventional power sources coinciding with a peak in renewable energy production due to a particular weather pattern. While it could be instinctively assumed that the conventional power plant could simply be switched off, or at least turned down and energy demands met from the renewable sources, in practice this is not possible as conventional fossil fuel power plants and nuclear plants cannot be quickly shut down and restarted; thus, it is the renewable energy source that often must be curtailed such that all the energy they can produce is not exploited. For example, in 2019 in California, 961 GWh of solar and wind energy was curtailed representing slightly over 2% of renewable production [1]. Integration of energy storage with renewable energy sources would enable all energy produced by a renewable energy source to be exploited, thus reducing the dependency on conventional, polluting sources of power. Flexible energy storage is a barrier to greater penetration and development of renewables. It can be seen from Fig. 24.2 that only around 0.5% of renewable energy capacity can be stored, though it is doubtless that these figures mask significant regional variations.

Energy storage is already a fundamental concept in the global energy economy. Hydrocarbons are currently the most exploited source of energy, accounting for more than 85% of global energy production [2]. What we consider our most familiar fuels: gasoline, coal, and natural gas, to name but a few, are energy storage media themselves. Many millions of years ago, the energy of the sun was consumed by plants enabling their growth and proliferation across the prehistoric earth. These plants provided a rich and plentiful food source for our dinosaur ancestors and as these prehistoric plants and animals died and were covered by millennia of new growth, they were slowly transformed into the fossil fuels we exploit today. Thus, energy storage is a concept that has existed for many millennia, but the fuels are literally fossils.

Storing Energy. https://doi.org/10.1016/B978-0-12-824510-1.00015-5
Copyright © 2022 Elsevier Inc. All rights reserved.

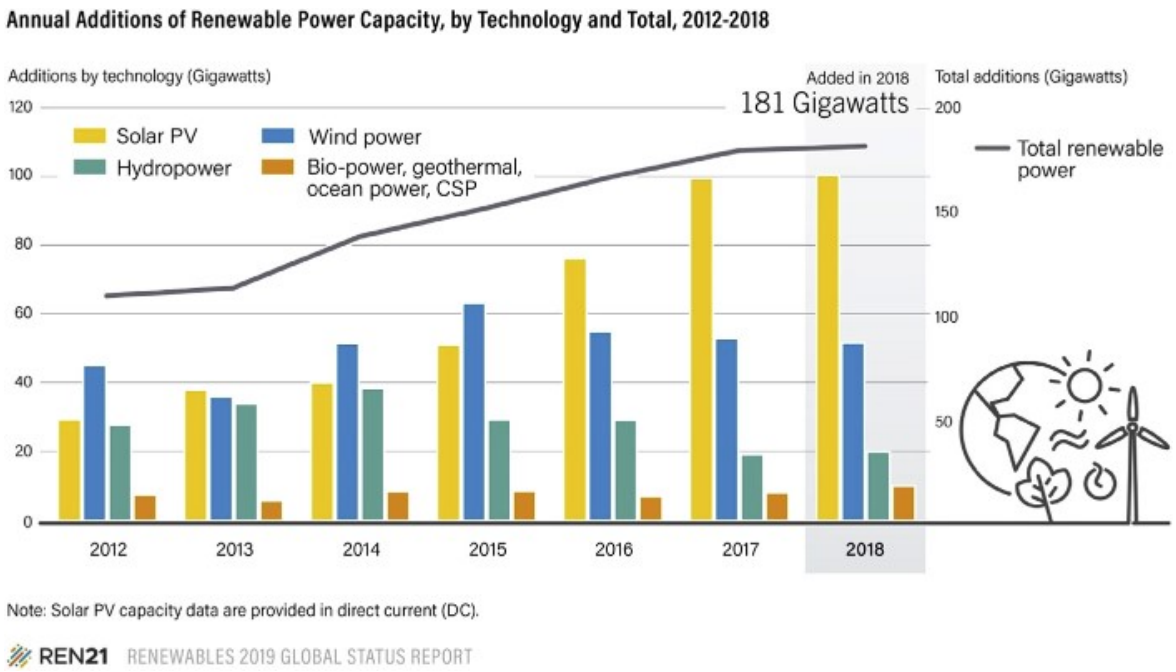

Figure 24.1 Annual additions of renewable power capacity by technology and total, 2012–18.

The challenges facing scientists and engineers developing new technologies for energy storage are twofold. Firstly, one must consider the environmental impact of the energy storage medium. While hydrocarbons provide a rich source of energy, the products of the combustion processes required to release the stored energy contribute to climate change, unless the carbon could be captured to produce a closed-carbon-cycle. Secondly, one must consider timescale. As stated above, the life cycle of organic life and its subsequent decomposition into a useable fuel source is extremely slow, taking many millions of years. Thus, when selecting a new energy storage medium, the ideal candidate should be able to release stored energy without producing any pollutants or harmful side products and should be able to store energy on an instantaneous timescale. Considering the fundamental requirements of energy storage, namely nonpolluting and quickly responding, hydrogen is a perfect medium for energy storage.

Hydrogen is not found in appreciable or exploitable concentrations freely on earth and instead must be produced from other compounds. There are two principal routes to the production of hydrogen. Most commonly hydrogen is produced from natural gas, via a process known as *steam reforming*. In addition to hydrogen, this process also produces carbon dioxide and is not a viable solution to the pollution-free production of hydrogen from excess renewable energy. Hydrogen may also be produced via electrolysis of water. In this process electricity (*electro-*) is used to break down (*-lysis*) water, H_2O, into its component parts of oxygen and hydrogen with no harmful or polluting side products. If the electricity required to carry out this process is provided by a renewable source, then a nonpolluting sustainable source of hydrogen is obtained. Release of the energy stored in hydrogen is an extremely clean process, producing only water as a byproduct and releasing large quantities of energy in doing so. Indeed, on a weight-by-weight basis hydrogen produces almost four times more energy than the equivalent weight of gasoline [3].

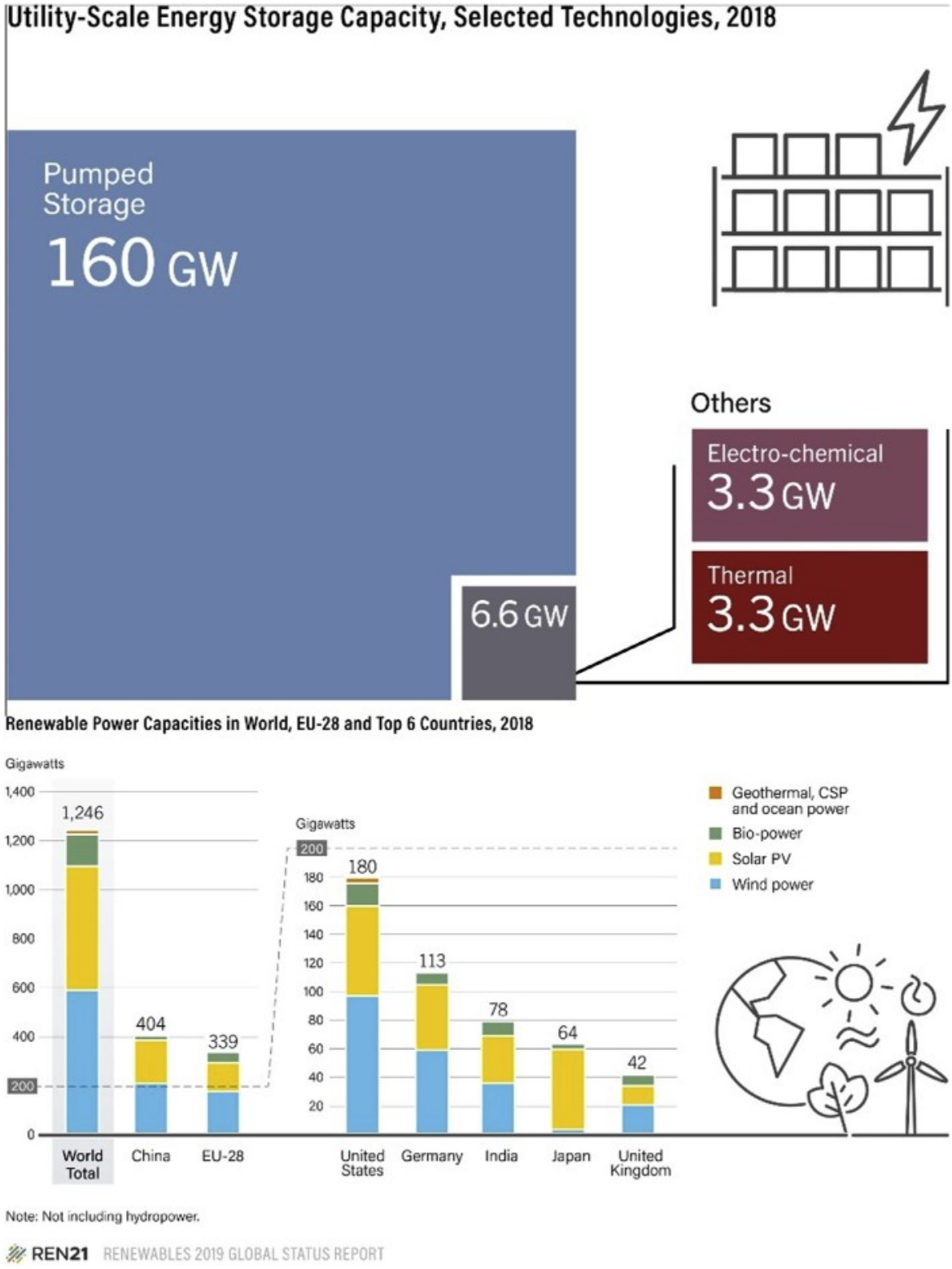

Figure 24.2 Energy storage and installed renewable capacity.

2. Hydrogen as an energy vector and basic principles of water electrolysis

2.1 Hydrogen as an energy vector

Hydrogen is a gaseous element occurring as its diatomic gas H_2. For clarity when this chapter refers to hydrogen, unless otherwise noted this refers to the diatomic molecule H_2. Since hydrogen does not naturally occur on earth it must be formed by the decomposition of other molecules. Approximately 95% of the hydrogen produced (around 50 million tonnes per annum) [4] is produced via steam reforming of natural gas and subsequent water-gas shift reaction (Scheme 24.1) with the remainder being formed via electrolysis. As can be seen from Scheme 24.1, the formation of hydrogen from natural gas results in the production of carbon dioxide. Given the finite supplies of natural gas and the greenhouse effect of carbon dioxide, production of hydrogen from this route does not address the needs of renewable energy storage. The production of hydrogen from water via electrolysis is a clean process, resulting in only oxygen being produced as a byproduct. If the electricity required to split the water into hydrogen and oxygen is supplied via a renewable energy source, then the process is environmentally benign.

Hydrogen has two main applications as an energy vector. Firstly, it may be combusted in a similar manner to natural gas. This is an extremely clean combustion process with water being the only product. A subset of this application is the storage of hydrogen in a conventional natural gas network, in a so-called power-to-gas process. This natural gas/hydrogen mixture is then combusted in an identical manner to unadulterated natural gas. It is worth noting that the coal gas that used to supply gas to many homes and industries could contain up to 50% hydrogen. Natural gas supplies now largely supplant coal gas. In addition to combustion, hydrogen may also be exploited as an energy vector via catalytic recombination with oxygen. In contrast to the thermal energy produced in a combustion process, the catalytic reaction with oxygen produces electrical energy. This process is exploited by fuel cells to produce electrical energy.

2.2 History of water electrolysis

Water electrolysis was first demonstrated in 1789 by the Dutch merchants Jan Rudolph Deiman and Adriaan Paets van Troostwijk using an electrostatic generator to produce an electrostatic discharge between two gold electrodes immersed in water [5].

Steam methane reforming

$$CH_4 + H_2O \longrightarrow CO + 3H_2$$

Water-gas shift reaction

$$CO + H_2O \longrightarrow CO_2 + H_2$$

Scheme 24.1 Production of hydrogen from natural gas.

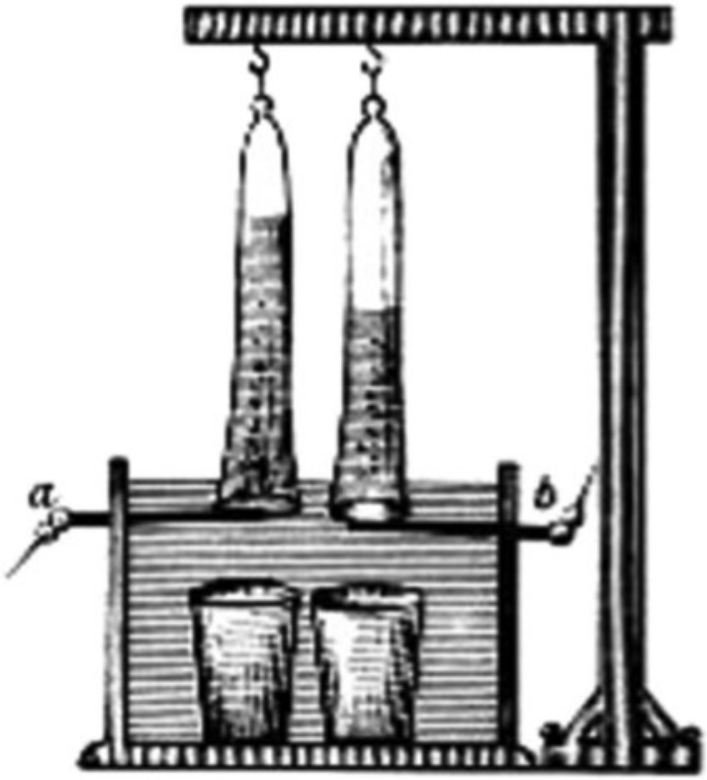

Figure 24.3 Ritter's electrolysis apparatus.

Later developments by Johann Wilhelm Ritter exploited Volta's battery technology and allowed separation of the product gases (Fig. 24.3) [6].

Almost a century later, in 1888, a method of industrial synthesis of hydrogen and oxygen via electrolysis was developed by the Russian engineer Dmitry Lachinov [7] and by 1902 more than 400 industrial water electrolyzers were in operation [8]. Early electrolyzers utilized aqueous alkaline solutions as their electrolytes, and this technology persists to this day. A more recent development in water electrolysis is the proton exchange membrane process, first described in the mid-1960s by General Electric as a method for producing oxygen for the Gemini Space Program [9]. Today several companies are active in the manufacture and development of electrolysis technologies, with NEL Hydrogen, Cummins, Giner ELX, and ITM Power being leaders in the field.

2.3 Electrochemistry and thermodynamics

The electrolysis of water is thermodynamically disfavored and as such requires an input of energy to drive the process. In the case of the electrolytic splitting of water into hydrogen and oxygen, this energy input comes in the form of a potential difference between the anode and cathode of an electrochemical cell. By application of Gibb's Free Energy equation (Eq. 24.1) and knowledge of the standard enthalpy of formation (286.03/kJmol) and ideal gas entropy (0.163/kJmol/K) of gaseous water we can calculate the free energy of water at 298 K (25°C).

$$\begin{aligned}\Delta G^{\circ} &= \Delta H^{\circ} - T\Delta S^{\circ} \\ \Delta G^{\circ} &= 286.03 - (298 * 0.163) \\ \Delta G^{\circ} &= 237.46/\text{kJmol}\end{aligned} \tag{24.1}$$

Eq. (24.1): Gibbs Free Energy

Using this free energy, we can calculate the reversible voltage required to split water electrolytically (Eq. 24.2), where n is the number of electrons transferred and F is Faraday's constant. Two electrons are required to produce a single molecule of hydrogen, hence $n = 2$.

$$\begin{aligned}V_{rev} &= -\frac{\Delta G^{\circ}}{nF} \\ V_{rev} &= -\frac{237,460}{2 \times 96,485} \\ V_{rev} &= -1.23\ V\end{aligned} \tag{24.2}$$

Eq. (24.2): Calculation of *Vrev*

This value of 1.23 V requires that all components be in the gaseous state, i.e., that the water which is consumed in the reaction be vaporized. In a conventional electrolyzer where water is at atmospheric pressure and temperatures are typically below 80°C there is an additional energy input required as illustrated in Eq. (24.3) where ΔH^{o} is equal to ΔG^{o} plus the energy required to vaporize water. This gives rise to the thermoneutral potential of 1.48 V. The potential at which water splitting occurs can approach the reversible potential by carrying out the electrolysis at high temperature and pressure and approaches to this will be discussed in Section 4.3.

$$\begin{aligned}V_{tn} &= -\frac{\Delta H^{\circ}}{nF} \\ V_{rev} &= -\frac{286,030}{2 \times 96485} \\ V_{rev} &= -1.48\ V\end{aligned} \tag{24.3}$$

Eq. (24.3): Calculation of *Vtn*

Two further concepts are required to understand the electrochemistry of an electrolyzer: overpotential and efficiency. While the electrolysis of water is thermodynamically feasible at 1.48 V, the reaction will occur prohibitively slowly, and a further potential must be applied to accelerate the reaction to a practical rate. This extra potential is known as the *overpotential* and minimizing this additional potential is fundamental in producing efficient electrolytic cells. The overpotential is due to a combination of the very low conductivity of water and the high activation energy required to split water. The former may be addressed by incorporating salts, acids, or bases into the water to improve its conductivity. This is the case with an alkaline

electrolyzer where the electrolyte is aqueous sodium hydroxide solution. The latter is addressed by the addition of suitable electrocatalysts, a concept considered in more detail in Section 25.3.

The efficiency of an electrolysis process can be considered in two ways. We can consider the Faradaic efficiency—the ratio of the number of moles of hydrogen produced versus the charge passed. If the process has a 100% Faradaic efficiency, then every electron produced by the oxidation of water is transferred to a corresponding proton to produce hydrogen. Note that two electrons are required to produce a single mole of hydrogen ($n = 2$, Eq. 24.2). The actual Faradaic efficiency may approach 100% but is always slightly lower due to parasitic electrochemical processes, e.g., degradation of components of the electrochemical cell; and the crossover of hydrogen to the oxygen producing side of the cell.

We can also consider the energy efficiency of the cell or stack. This is measured by calculation of the energy available from the hydrogen produced by the cell, using the higher heating value of hydrogen [10] and dividing this by the energy consumed by the cell as shown in Eq. (24.4), where I is the cell current, V is the voltage, and t is the time over which the hydrogen production was measured.

$$\eta_{eff} = \frac{\text{no. of moles of hydrogen produced} \times HHV_{H_2}}{I \times V \times t} \tag{24.4}$$

Eq. (24.4): Calculation of cell energy efficiency.

Commercial electrolyzers often express their energy efficiency in terms of the whole system, η_{sys}, including parasitic loads due to pumps, heaters, etc. This is commonly expressed in kWh/Nm^3 of hydrogen produced, for example, the C30 electrolyzer from NEL hydrogen requires 5.8 kWh/Nm^3 of hydrogen giving a system efficiency of 60%.

The individual reactions taking place during electrolysis differ depending on the nature of the process taking place and will be discussed in full in Section 3.

3. Hydrogen production via water electrolysis

3.1 Water electrolysis

The basic principles, chemistry, and thermodynamics of water electrolysis have been described in Section 2. Herein we discuss the device architectures, their advantages and disadvantages, and materials of construction. There are three main routes to the electrolysis of water, alkaline electrolysis, proton exchange membrane (PEM) electrolysis, and solid-oxide electrolysis. Of these only alkaline and PEM electrolysis have been commercialized and while solid-oxide electrolyzers show great technological promise, they are still the subject of considerable development [11]. The technological parameters defining the main types of commercial electrolyzers are shown in Table 24.1 [12,13]. Comparable information on solid oxide electrolyzers is not available due to the lack of commercial devices.

Table 24.1 Comparison of water electrolysis methods.

	Alkaline electrolyzer	**Proton exchange (PEM) electrolyzer**
Cell temperature (°C)	60–80	50–80
Cell pressure (bar)	<30	<30
Current density (Acm^{-2})	0.2–0.4	0.6–2.0
Cell voltage (V)	1.8–2.4	1.8–2.2
Power density (Wcm^{-2})	<1	<4.4
Efficiency (HHV) (%)	62–82	67–82
Specific energy consumption stack (kWhN/m H_2)	4.2–5.9	4.2–5.6
Specific energy consumption system ($kWhNm^{-3}$ H_2)	4.5–7.0	4.5–7.5
Partial load range (%)	20–40	5–10
Cell area (m^2)	>4	<0.03
H_2 production rate ($Nm^{3/}h$)	<760	<10
Lifetime stack (h)	<90,000	<20,000
Lifetime system (y)	20–30	10–20
Degradation rate (μVh^{-1})	<3	<14

3.2 Alkaline water electrolysis

The first commercialized water electrolysis system was based on the principles of alkaline water electrolysis and alkaline-based systems remain the most ubiquitously utilized water electrolysis systems [14]. A schematic of an alkaline water electrolyzer is given in Fig. 24.4. The cathode and anode are often manufactured from nickel [15] and the separator between the anodic and cathodic chambers is a polymer which is permeable to hydroxide ions and water molecules, for example, Zirfon Perl from Agfa. Alkaline electrolyzers have the advantage of technological maturity and relatively low cost compared to PEM electrolyzers.

The reactions taking place in an alkaline electrolyzer are given in Scheme 24.2.

There are several technological disadvantages associated with the alkaline electrolysis system, namely low current density, limited ability to operate at low loads, and the inability to operate at high pressure. The latter two limitations are due to the crossover of gases possible through the separator. This will increase both with increasing pressure of hydrogen at the cathode and will also increase with reduced load where the oxygen production rate decreases and the hydrogen concentration in the oxygen stream can increase to dangerous levels (H_2 lower explosion limit >4%) [16].

3.3 Proton exchange membrane (PEM) electrolysis

A schematic of a PEM electrolyzer is given in Fig. 24.5. Central to the operation of the PEM electrolyzer is the proton conducting membrane. This membrane is made of a sulfonated fluorinated polymer. The most used membrane is Nafion, manufactured

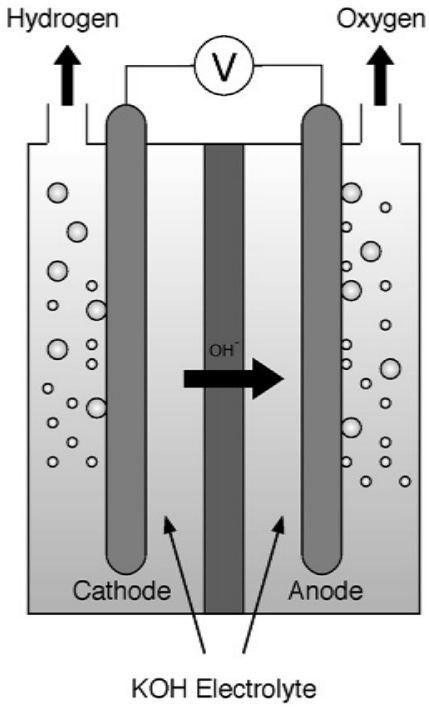

Figure 24.4 Alkaline water electrolyzer.

Cathode Reaction

$$2H_2O_{(l)} + 2e^- \longrightarrow H_{2(g)} + 2OH^-_{(aq)}$$

Anode Reaction

$$2OH^-_{(aq)} \longrightarrow H_2O + {}^1/_2O_{2(g)} + 2e^-$$

Scheme 24.2 Alkaline water electrolysis.

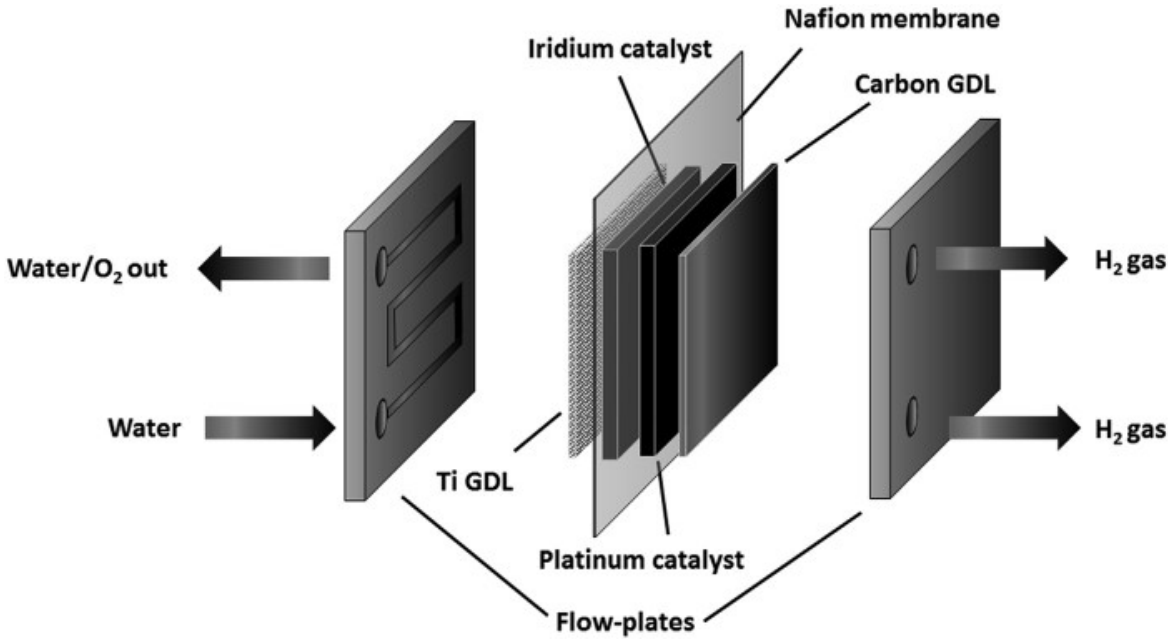

Figure 24.5 Cell layout diagram for a PEM electrolyzer.

by DuPont. Various thicknesses of Nafion may be employed ranging from 25 to 250 μm. The exact thickness of membrane required for any specific application is determined by the conditions to be employed in the electrolyzer. Higher pressures and conditions likely to degrade the membrane at a greater rate, e.g., low load operation or frequent stop-starts requires a thicker membrane either to withstand the high differential pressure and minimize gas crossover or to provide a suitable margin for material loss due to degradation. The thinner the membrane, the greater the efficiency of the electrolysis process. This is due to a reduction in the resistance of the membrane with decreasing thickness [17,18]. Thus, a balancing act must be struck between the optimal electrochemical properties of the membrane and its suitability for a given set of process conditions. There is considerable ongoing research into the development of new membranes with improved properties including greater proton conductivity and improved mechanical strength [19,20].

As discussed in Section 2, the kinetics of water oxidation are extremely slow without the addition of suitable electrocatalysts. Due to the highly acidic nature of the PEM electrolysis process, the choice of catalysts is limited to rare transition metals that are stable in acidic conditions for example, rhodium, ruthenium, platinum, iridium, and their oxides [21]. The current state-of-the-art for electrocatalysts in PEM water electrolysis is platinum at the cathode for proton reduction and iridium oxide at the anode for water oxidation. There is a large amount of research undertaken to prepare new electrocatalysts for both water oxidation and proton reduction [22–30] to increase the efficiency of the process and to reduce cost. The combination of the membrane and the electrocatalysts is collectively known as the *membrane electrode assembly (MEA)*.

The water is fed into the anode of the electrolyzer and the product gases are conducted away from the reactive sites on the MEA via the flow channels of the bipolar flow plates. These flow plates are typically manufactured from titanium as this gives the mechanical strength and resistance to corrosion required. Stainless steel and graphite are also used in some systems though their application is limited by relatively poor corrosion properties and the poor mechanical strength of graphite compared to titanium. Despite titanium's near ubiquitous use, it is not the perfect material for bipolar plates. It is subject to oxidation and is very difficult to machine, adding to its cost. There is limited research into alternative materials. A recent publication described the use of 3D printing to prepare flow plates though the difficulty of rendering these plates suitably conductive limits their current use to prototyping [31].

Between the flow fields of the bipolar plates and the MEA, a conductive layer is added. This layer is known as the *gas diffusion layer (GDL)* and is added to improve the electrical connection between the bipolar plates and the MEA and to ensure the effective mass transport of both the reactant water and the product gases. The cathodic GDL is often made of carbon paper. This material is not suitable for use at the anode as the highly oxidative conditions at this electrode would quickly decompose the carbon paper. Instead, a titanium or similar inert metal mesh is inserted between the flow fields and the MEA.

The reactions taking place in a PEM electrolyzer are given in Scheme 24.3.

Cathode Reaction

$$2H^{+}_{(aq)} + 2e^{-} \longrightarrow H_{2(g)}$$

Anode Reaction

$$H_2O_{(l)} \longrightarrow {}^{1}/_{2}O_{2(g)} + 2H^{+}_{(aq)} + 2e^{-}$$

Scheme 24.3 PEM water electrolysis.

3.4 Solid-oxide water electrolysis

Solid-oxide electrolysis differs from both alkaline and PEM systems in that the operating temperature is typically an order of magnitude greater in a solid oxide electrolyzer (SOE), spanning the range 800−1000°C. At this temperature it should be apparent that the feed cannot be water and in this case the electrolyzer is fed with steam. The chemical reactions taking place in the SOE are given in Scheme 24.4.

Intuitively the high operating temperatures of the SOE system would suggest that the efficiency of operation would be poor; however, this is not the case. The increase in thermal energy demand is compensated for by the decrease in the electrical energy demand and the overall energy demand of the system is largely insensitive to increasing the temperature. This is illustrated in Fig. 24.6 [32].

In the solid-oxide electrolysis process, water in the form of high-pressure steam is reduced at the cathode to give hydrogen gas and oxygen anions. These anions migrate through the solid-oxide electrolyte, where they are oxidized on the anode to produce oxygen gas. The electrons produced from the oxidation travel around the external circuit and supply the electrons for the water reduction. The product gases diffuse through the porous electrodes. A schematic of the SOE is given in Fig. 24.7 [33].

The SOE utilizes a solid electrolyte separating the anode and the cathode. In this regard the system has some similarity with the PEM system, where a solid electrolyte is also employed to provide the ionic conductivity to the system. The current state-of-the-art electrolyte in a solid-oxide system is yttria-stabilized zirconia (YSZ) [32]. This material only has sufficient ionic conductivity at high temperatures; hence the requirement to operate at temperatures approaching 1000°C. At this high temperature, there are numerous problems with cell integrity including poor long-term cell stability, interlayer diffusion, fabrication and materials problems [34]. In addition to oxygen anion conductivity, it is also possible to operate an SOE on the principle of proton

Cathode Reaction

$$H_2O_{(l)} + 2e^{-} \longrightarrow H_{2(g)} + O^{2-}_{(aq)}$$

Anode Reaction

$$O^{2-}_{(aq)} \longrightarrow {}^{1}/_{2}O_{2(g)} + 2e^{-}$$

Scheme 24.4 Solid-oxide electrolyzer water electrolysis.

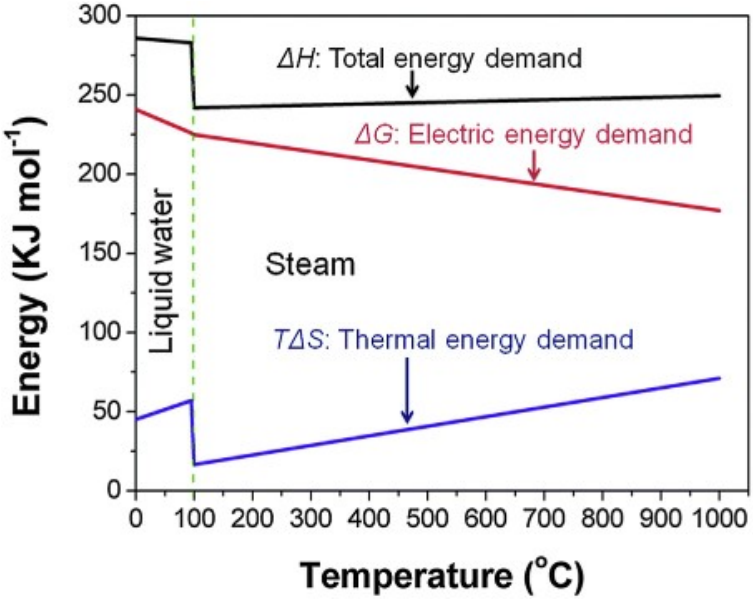

Figure 24.6 Electrolysis energy demand.
Reproduced from Ref. L. Bi, S. Boulfrad, E. Traversa, Chem. Soc. Rev. 43 (2014) 8255–8270 with permission from the Royal Society of Chemistry.

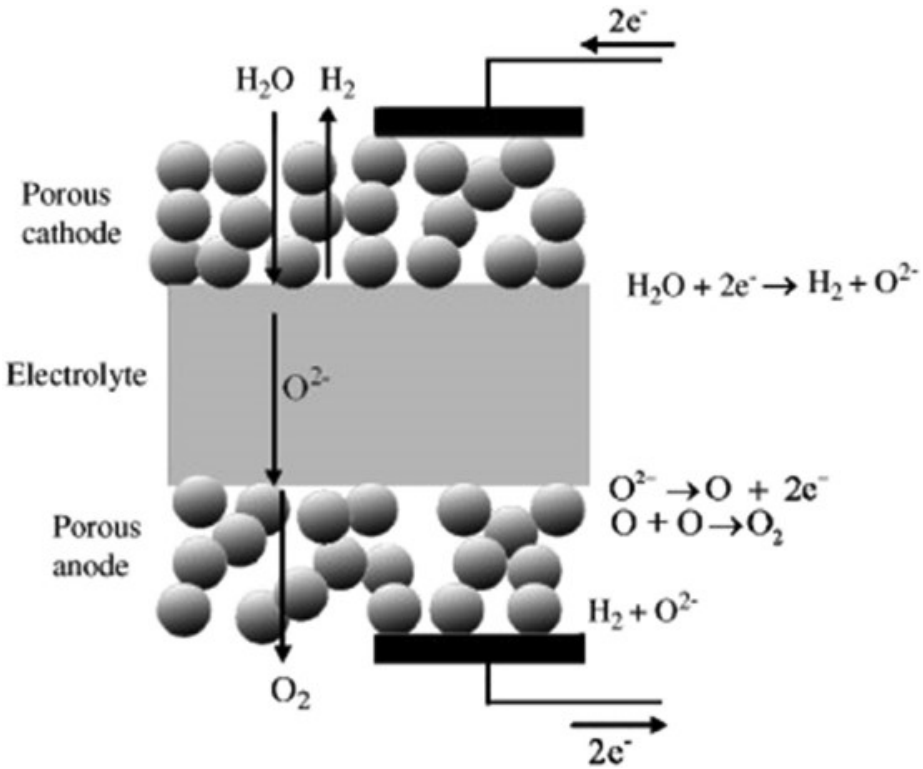

Figure 24.7 Solid-oxide electrolyzer (SOE) operation.
Reprinted from M. Ni, M. Leung, D. Leung, Technological development of hydrogen production by solid oxide electrolyser cell, Int. J. Hydrog. Energy 33 (2008) 2337–2354, Copyright (2008), with permission from Elsevier.

conductivity in a manner similar to a PEM electrolyzer [35]. In this system a different electrolyte must be adopted. Doped $BaCeO_3$ shows good conductivity in this system [36].

4. Strategies for storing energy in hydrogen

4.1 Properties of hydrogen related to storage

Hydrogen was first identified as an element by Henry Cavendish in 1766 during a series of experiments wherein he added various metals to strong acids. He described the gas produced as inflammable air. The primitive apparatus used by Cavendish to first isolate and store hydrogen gas is shown in Fig. 24.8 [37]. Since this first isolation of hydrogen, considerable effort has gone into the development of suitable storage technologies for containing this gas. Storage by compression or via cryogenic liquefaction are the most developed technologies and form the basis of the technologies used in current automotive demonstration projects. A significant challenge associated with both pressurized and cryogenic storage is that the storage vessel itself contributes at least 90% to the total system weight [38].

Basic properties of hydrogen are given in Table 24.2.

Hydrogen has the highest energy density by weight of any fuel; however, due to its very low density, its volumetric energy density is very poor. Thus, storage of large quantities of energy in the form of uncompressed hydrogen gas would require impractically large storage facilities. This requirement may be addressed by compression or liquefaction of the hydrogen, thus increasing its volumetric energy density.

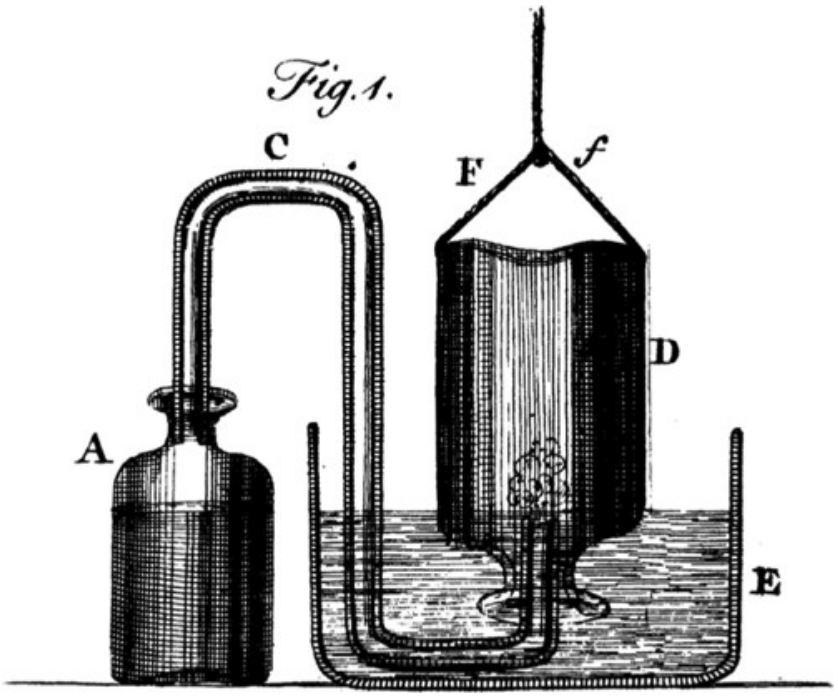

Figure 24.8 Cavendish apparatus for isolation of hydrogen gas.

Table 24.2 Hydrogen properties.

Property	Value	Unit
Melting point	13.99	K
Boiling point	20.27	K
Density	0.0899	g/L
Higher heating value	141.80	MJ/kg
Lower heating value	119.96	MJ/kg
Gravimetric (specific) energy density	141.80	MJ/kg
Volumetric energy density @ STP	0.0107	MJ/L

4.2 Gaseous hydrogen storage

When considering a storage strategy for hydrogen, it is important to consider the final application of the hydrogen and to match the pressure of the storage medium to that required by the application. The compression of hydrogen to a suitable storage pressure consumes energy and consequently incurs an efficiency penalty. Compression of hydrogen to 350–700 bar consumes energy equal to 5%–20% of the lower heating value of hydrogen. These pressure ranges are considered the optimum for transport applications using compressed hydrogen, as they represent a balance between compression energy consumption, driving range of the vehicle being fueled, and the investment required in refueling stations and associated infrastructure [39]. Research and development into the storage of pressurized gaseous hydrogen is largely predicated on the emergence of a hydrogen vehicle and refueling sector. The United States Department of Energy (DoE) has produced a series of targets for the storage of hydrogen (Table 24.3) [40].

The "Ultimate" target represents the performance that is anticipated to be required for full penetration of hydrogen powered vehicles into the light-duty market. In addition to the energy density requirements outlined above, there are also technical requirements related to the small size of the hydrogen molecule. This gives hydrogen a high diffusivity in many materials. In the case of storage of high pressure hydrogen in steel containers, this diffusivity can result in embrittlement of the container leading to failure of the material [41–45]. The targets set by the DoE and the challenges of embrittlement have driven a great deal of research in the storage of hydrogen as a high-pressure gas.

Table 24.3 DoE hydrogen storage targets.

Target	2020	2025	Ultimate
System gravimetric capacity (kWh/kg)	1.5	1.8	2.2
System volumetric capacity (kWh/L)	1.0	1.3	1.7
System fill time for 5-kg fill (min)	3–5	3–5	3–5

In vehicular applications, two storage vessel technologies known as *Type III* and *Type IV* have grown to a dominant position in vehicular applications [46]. Type III storage vessels are composed of a pressure vessel made of a metallic liner fully wrapped with a fiber-resin composite [47,48]. Type IV storage vessels differ from type III vessels in that the pressure vessel is made of a polymeric liner as opposed to a metallic liner, and is again fully wrapped with a fiber-resin composite [47,48]. Type III storage vessels are the technically superior design due to the metallic liner. This liner gives the storage vessel a higher thermal conductivity which minimizes the temperature rise associated with the filling of the storage vessel with compressed hydrogen. High cost remains the most significant barrier to successful implementation of this technology, though public perception of the safety of compressed hydrogen storage may also need to be overcome [49,50].

4.3 Cryogenic liquid hydrogen storage

Conversion of hydrogen to a cryogenic liquid requires a large input of energy to condense the gas. This energy input amounts to 30%–40% of the lower heating value of hydrogen and results in a corresponding loss of efficiency in any system relying on cryogenic hydrogen [46]. On this basis it compares poorly with storage of hydrogen as a pressurized gas despite the increase in volumetric energy density to 8 MJ/L. In addition, storage containers for cryogenic hydrogen must be insulated and refrigerated to maintain the low temperature required and require frequent venting to allow evaporated hydrogen gas to escape.

4.4 Cryocompressed hydrogen storage

Cryocompression of hydrogen refers to several different storage methods that combine elements of compressed and cryogenic storage and includes liquid hydrogen, cold compressed hydrogen, or hydrogen stored as a mixture of saturated liquid and vapor. Common between methods is the storage of hydrogen in its cryo-state and at pressures of 250–350 bar [51]. Storage of hydrogen as a cryocompressed fluid serves to overcome the limitations of both compressed gas and cryogenic liquid storage allowing both an increase in volumetric energy density versus compressed gaseous hydrogen and also minimizing the evaporative losses associated with cryostorage at atmospheric pressure [52].

4.5 Hydrogen storage by physisorption

Non-mechanical means can be used to store hydrogen, for example, by physisorption onto porous supports. This process is reversible, and the hydrogen may be adsorbed and desorbed over multiple cycles. The hydrogen is physically attached to the adsorbent via van der Waals interactions and is limited to a monolayer of hydrogen. Sorbents with high surface areas therefore have the greatest capacity for hydrogen

Table 24.4 Properties of selected physisorption media.

Storage medium	Temperature (°C)	Pressure (bar)	Capacity (wt%)	Reference
Carbon nanotubes	27	1	0.2	[57]
	25	500	2.7	[58]
	−196	1	2.8	[59]
Graphene oxide	25	50	2.6	[60]
Polymers of intrinsic microporosity	−196	10	2.7	[61]
Hyper cross-linked polymers	−196	15	3.7	[62]
Covalent organic frameworks	−196	70	7.2	[63]
Zeolites	25	100	1.6	[64]
	−196	16	2.07	[65]
Metal organic frameworks	25	50	8	[66]
	−196	70	16.4	[67]
Clathrate hydrates	−3	120	4	[68]

Reproduced from Ref. A.F. Dalebrook, W. Gan, M. Grasemann, S. Moret, G. Laurenczy, Chem. Commun. 49 (2013) 8735–8751 with permission from the Royal Society of Chemistry.

storage [53]. Cryogenic hydrogen absorption at temperatures below −195°C can profoundly increase the level of physisorption of hydrogen [54,55]. The absorbent properties of various materials are given in Table 24.4 [56].

4.6 Hydrogen storage by chemisorption

In contrast to hydrogen storage by physisorption, chemisorption of hydrogen requires that the hydrogen undergo a chemical transformation and become chemically bonded to another species. The increased energy density in chemisorbed hydrogen is attributed to the shorter mean distance between hydrogen atoms in the hydride compared with the hydrogen molecules in a compressed or liquefied state (Fig. 24.9) [39]. The advantage of this approach is the very high energy density achievable compared to storage of hydrogen in compressed or liquefied form. In common with other hydrogen storage methods, storage via chemisorption has its share of technical challenges, namely ease and cyclability of charging and discharging, storage capacity, and stability of the material after charging [56]. From a practical perspective if one were to consider a system wherein pressurized hydrogen was pumped at pressure onto a discharged hydrogen precursor, formation of the hydride would have a given heat of formation, ΔH, associated with it. If the tank is to be filled with hydrogen in the 3 min filling time proposed by the DoE (Table 24.3), a great deal of heat would require to be dissipated in a very short time requiring a prohibitively large heat exchanger to be installed into the storage tank.

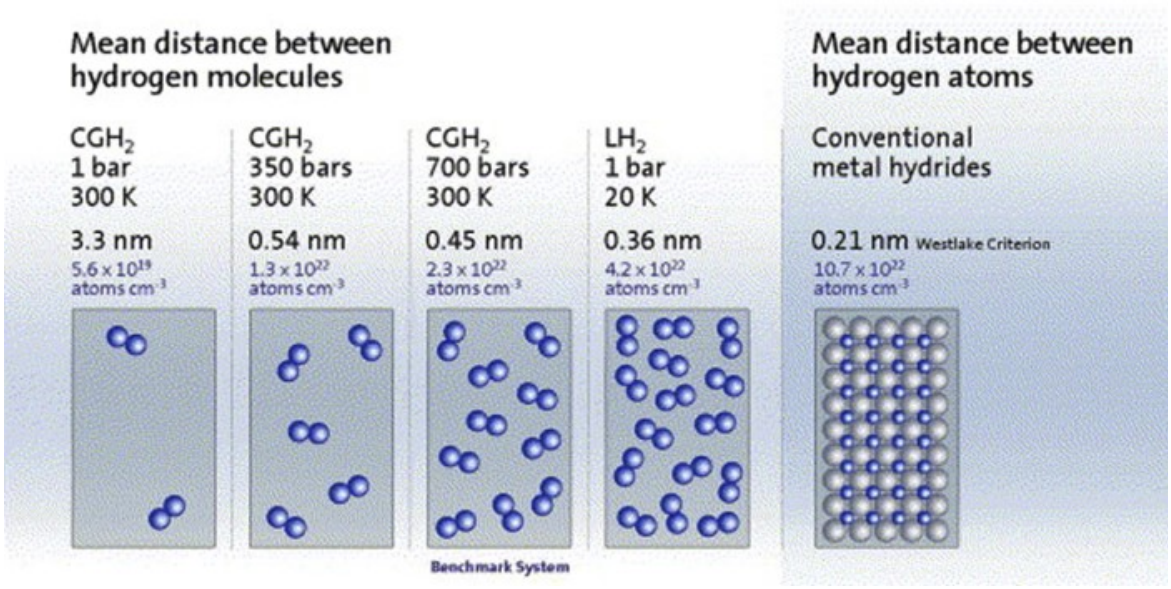

Figure 24.9 Mean distance between hydrogen molecules.
Reprinted from R. von Helmolt, U. Eberle, Fuel cell vehicles: Status 2007, J. Power Sources 165 (2007) 833–843 Copyright, with permission from Elsevier.

While there are clearly several technical challenges to be overcome in relation to the use of hydrides as a hydrogen storage medium, there are several candidates undergoing detailed development to overcome these limitations. Current research is focused on metal hydrides based on alkali and alkaline earth elements such as MgH_2 [69] and complex hydrides such as $NaAlH_4$ [70], the borohydrides $LiBH_4$ [71,72] and $NaBH_4$ [72], and $LiNH_2$ [73].

Storage capacities of various metal hydrides and equivalent materials are given in Table 24.5 [74].

4.7 Power to gas

Power to gas describes the injection of either hydrogen directly produced via electrolysis and suitably purified if required or methane produced via methanation of hydrogen into the natural gas network. This topic is described in more detail elsewhere in this volume and is considered here only briefly for completeness. The adulteration of methane with hydrogen gas is well known historically. "Town gas" derived from coal comprising a mixture of hydrogen, carbon monoxide, and methane was supplied to industrial and domestic properties from the 1840s and was only phased out in the UK with introduction of natural gas sourced from the North Sea. The potential of the natural gas network, ubiquitous in all developed countries, has tremendous potential as a storage medium for energy. In the UK alone, more than 836,000 GWh of energy were consumed in the form of natural gas in 2011 [80]. Even small amounts of hydrogen gas stored in this network amount to a large amount of energy storage.

There are limitations to the storage of hydrogen in the natural gas network. Due to the potential for hydrogen embrittlement as discussed in relation to pressurized

Table 24.5 Hydrogen storage capacities.

Storage medium	Capacity (wt%)	Operating temperature (°C)	Reference
LiH	12.6	720	[75]
NaH	4.2	425	[75]
KH	3.5	250–330	[70]
BeH_2	18.16	250	[76]
MgH_2	7.69	327	[69]
CaH_2	4.8	600	[76]
$LiAlH_4$	10.54	190	[77]
$NaAlH_4$	7.4	200	[70]
$LiNH_2$	6	372–400	[78]
KNH_2	3.66	338	[79]
$NaNH_2$	5.15	210	[77]
$LiBH_4$	18.5	400	[71]
$NaBH_4$	10.6	240–450	[72]

Reprinted from H. Jindal, A.S. Oberoi, I.S. Sandhu, M. Chitkara, Potential porous mediums for electrochemical hydrogen storage: State of the art and comparative study, Mater. Today Proc. (2020) 1888–98, Copyright, with permission from Elsevier.

Scheme 24.5 Methanation of hydrogen.

hydrogen storage above, and the different burning characteristics of methane/hydrogen mixtures compared to pure methane [81] limitations are placed on the quantity of hydrogen in natural gas, for example, 0.1% by mole in the UK [82]. This limitation in the quantity of hydrogen that can be stored in the gas network can be overcome by conversion of the hydrogen to methane via reaction with carbon dioxide or carbon monoxide (Scheme 24.5) [83,84] in a process known as *methanation*.

5. Technology demonstrations utilizing hydrogen as an energy storage medium

5.1 System engineering

A block diagram of a generic energy storage system using hydrogen as the energy storage medium is given in Fig. 24.10.

The energy source for such an energy storage system is typically a renewable source such as wind or photovoltaic though in principle any source of electrical energy may be used, even grid electricity if economics are appropriate, for example, if very cheap grid electricity can be sourced during off-peak periods. The power conditioning

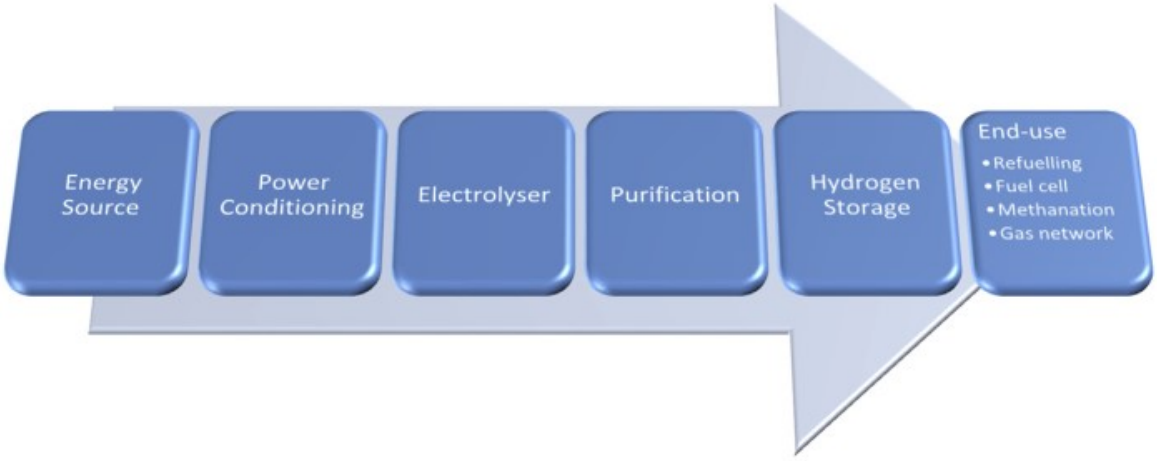

Figure 24.10 Block diagram of hydrogen-based renewable energy storage.

section of the system is of paramount importance and will determine whether electricity is taken from the energy source, the voltage of that electricity, and whether it should be sent directly to the electrolzser or whether it should be stored in an intermediate energy store, for example, a battery. The use of a battery in the power conditioning step can help to overcome limitations in the performance of an electrolyzer at low loads and to minimize start/stop cycling which can decrease the life time of the electrolyzer. Alkaline electrolyzers, in particular, have minimum loads typically around 20%–40% of full load [12]. PEM electrolyzers have much better low load performance but at low loads gas crossover increases [85] as well as the degradation rate of the membrane [18]. The choice of electrolyzer type, alkaline, PEM, or SOE, will be based on the economic and technical aspects of the project. The characteristics of each type of electrolyzer are discussed in Section 3.

Hydrogen gas produced by an electrolyzer can be of varying purity depending on both the type of electrolyzer and the operating conditions employed. The two significant impurities found in the hydrogen gas stream from an electrolyzer are water and oxygen. Water is often removed by passage of the gas through a desiccant, e.g., silica gel, by pressure swing adsorption or a combination of both. Removal of oxygen is via a catalytic recombination process wherein the oxygen is recombined with hydrogen to produce water. This process is carried out by passage of the product gas through a palladium filter heated to 300–600°C depending on the exact composition of the filter [86] or via catalytic recombination using palladium impregnated onto an alumina support [87]. It goes without saying that this should be placed upstream of the final drying process to prevent reintroducing water to the product gas. The parasitic load from this balance of plant will reduce the overall system efficiency. Contamination of the hydrogen with oxygen is typically at a lower level than the opposite case due to the greater size and lower mobility of the oxygen molecule within the membrane and the differential pressure between the hydrogen and oxygen producing sides of the membrane; however, despite being at a low level, oxygen contamination can reduce the purity of the product gas to a level where further purification is required, particularly for applications requiring high purity, for example, LED device manufacturing, silicon carbide epitaxy, and polysilicon manufacturing [88]. Hydrogen can be

contaminated by up to 2.7% oxygen at high pressure (*ca.* 130bar) [85]. While still outside the flammability limit for hydrogen/oxygen mixtures (3.9%–95.8%), a safety margin must be considered and any reading greater than 2% is likely to lead to an alarm condition. In addition, this crossover of gases increases the likelihood of recombination of oxygen and hydrogen within the membrane of the electrolyzer, which can lead to a reduction in the life time of the membrane and reduces the efficiency of the electrolyzer [89].

5.2 Renewable energy storage

The first hydrogen-based system for storing renewable electricity by means of electrolysis and subsequent hydrogen storage was realized in 1991 [90]. This project was based in Nuenberg Vorm Wald in Germany and marked the beginning of that country's leadership in the adoption and demonstration of technologies essential for the realization of the hydrogen economy. This pilot plant operated from 1991 to 1999 and utilized electrical power generated from an array of photovoltaic panels with a capacity of 266 kW_p (Fig. 24.11).

Over the life time of the project this demonstration plant utilized both alkaline (low and high pressure) and PEM electrolysis technologies (Fig. 24.12). This plant tested several subsystems connected to the electrolysis system including hydrogen and oxygen purification and storage systems, fuel cells, gas-fired boilers fueled with a hydrogen/methane mixture and a liquid hydrogen fueling station used to fuel prototype

Figure 24.11 Overhead view of the Nuenberg Vorm Wald Plant.
Reprinted from A. Szyszka, 10 Years of Solar Hydrogen Demonstration Project at Neunburg Vorm Wald, Germany, Int. J. Hydrog. Energy 23 (1998) 849–860, Copyright, with permission from Elsevier.

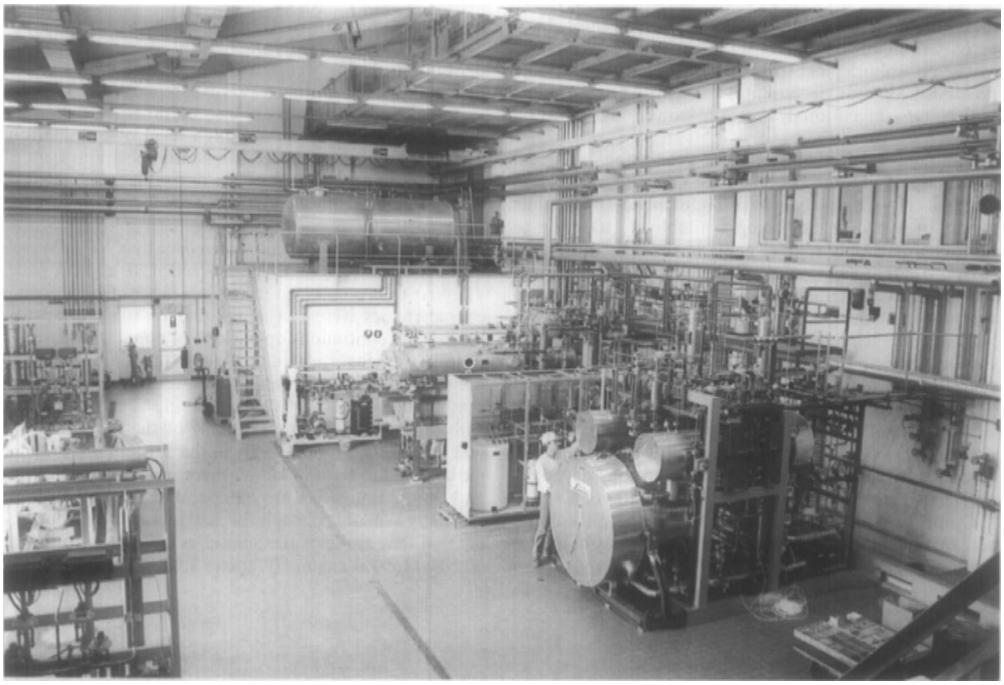

Figure 24.12 Interior of the Neunberg Plant—DI Water tank and low pressure electrolyzers (top right) and high pressure electrolyzer (bottom right).
Reprinted from A. Szyszka, Ten years of solar hydrogen demonstration project at Neunburg Vorm Wald, Germany, Int. J. Hydrog. Energy 23 (1998) 849–860, Copyright, with permission from Elsevier.

liquid hydrogen fueled cars. Regarding the latter, liquid hydrogen is no longer considered the technology of choice for exploiting hydrogen in transportation applications and has now been largely supplanted by pressurized hydrogen gas.

Since the pioneering work at Nuenberg (Fig. 24.12), many demonstration plants have followed and electrolyzers are scaling from megawatt (MW) to gigawatt (GW)-scale, as electrolyzer technology matures and develops (Fig. 24.13) [91].

Germany continues to be very active in developing green hydrogen projects. Amprion (transmission system operator) and OGE (gas network operator) have proposed the Hybridge project—a plan for a 100 MW electrolyzer and a dedicated hydrogen pipeline which is due to come online in 2023 [92]. A 10 MW electrolyzer is currently under construction at the Shell Rhineland Refinery in Wesseling, Germany. The PEM electrolyzer, built by ITM Power, will be the largest of its kind to be deployed on an industrial scale and will be used to produce more than 1000 tonnes of hydrogen per year, supplanting an equivalent amount currently produced by the carbon-intensive process of steam methane reforming (Scheme 24.1) [93].

The German government also approved 11 other hydrogen demonstration projects in 2019 (Table 24.6).

Outside of Germany, there are many other upscaling and demonstration projects underway, and we have attempted to highlight some of the key examples.

The GRHYD demonstration project supported by the French government was conducted by ENGIE and partners from 2014 to 2020, with the target of meeting 23% of its gross end-user energy consumption from renewable sources by 2020. The PEM

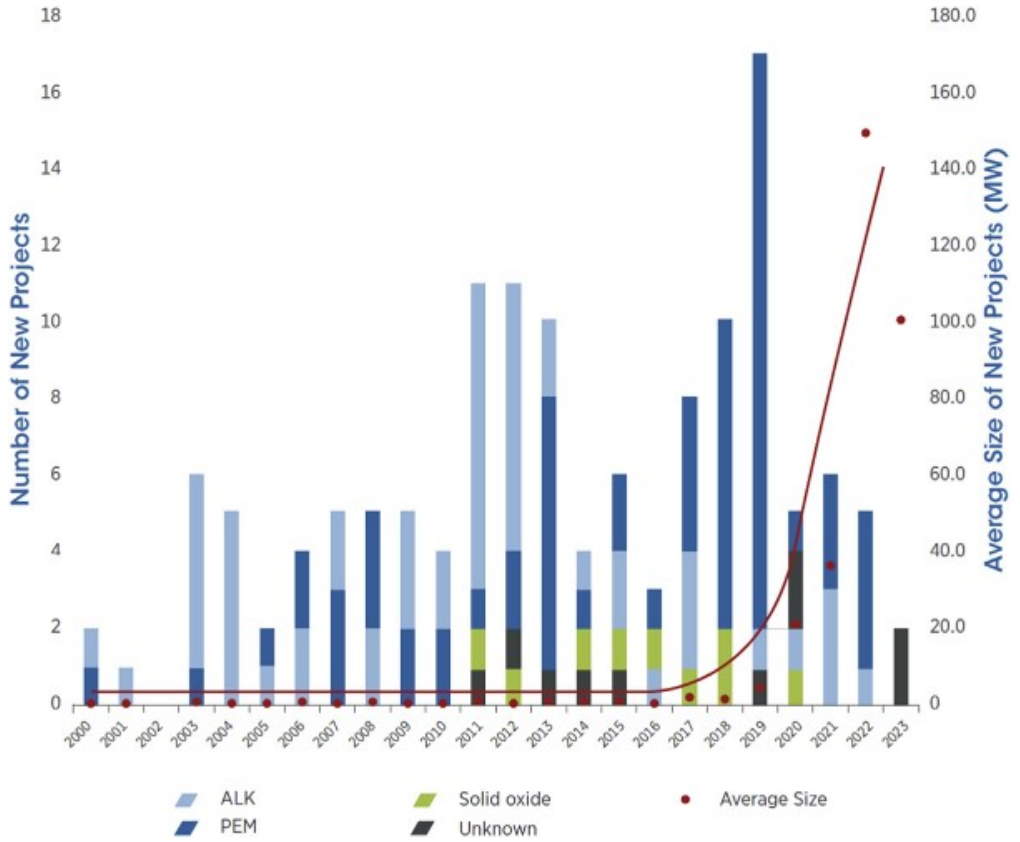

Figure 24.13 Timeline of power-to-hydrogen projects by electrolyzer technology. RENA (2019).

Table 24.6 German electrolyzer projects.

Project	Capacity (MW)	Purpose	Reference
CCU P2C salzbergen	Not reported	Synthetic methane production	[91]
DOW green MeOH	Not reported	Methanol production	[91]
Element eins	100	Power to gas	[94]
EnergieparkBL	35	Power to gas	[95]
GreenHydroChem	50	Power to gas	
H2 stahl	Not reported	Hydrogen injection into a blast furnace	[96]
H2 Whylen	10	Power to gas	[97]
HydroHub fenne	17.5	Power to gas	[98]
Norddeutsches reallabor	77	Vehicle refueling	[99]
RefLau	10	Storage and power	[100]
ReWest	10	Not reported	[91]

electrolyzer used in the project had a capacity of 10 Nm^3 of hydrogen per hour and storage was in metal hydrides. Over the course of the project 100 houses were provided with a mixture of hydrogen and natural gas for domestic heating. The proportion of hydrogen in the natural gas was increased over the course of the project from 2% to a maximum of 20% [101].

In northwestern Australia, Horizon Power aims to replace current diesel generators and wind turbines powering the town of Denham with a dedicated solar farm and electrolyzer for capturing any excess energy produced by the solar farm and storing this as hydrogen. This stored hydrogen will be utilized in a fuel cell for the generation of electricity, providing round the clock power from renewable supplies. The project will produce a minimum of 13,000 kgs of hydrogen per year supplying around 40% of the yearly electricity requirements to 100 residential properties. This project will be an example of the use of green hydrogen to provide baseload power generation to a community [102].

In the United States, the Department of Energy has multiple projects on hydrogen production, infrastructure, safety, and grid integration through their H2@Scale initiative, a project to advance hydrogen production, transport, storage, and use [103].

Japan has also developed a 10 MW electrolyzer combined with 20 MW of solar power generation facilities under the scheme of Fukushima Hydrogen Energy Research Field (FH2R) in a project led by Toshiba. Construction of the facility was completed in early 2020 and represents a substantial effort to integrate hydrogen into a range of current applications from transport to electricity generation and industrial use [104].

6. Emerging technologies and outlook

6.1 *Electron coupled proton buffers and decoupling of hydrogen gas generation*

An unavoidable consequence of electrolysis in a conventional electrolyzer is that the production of oxygen and hydrogen takes place in the same device separated only by a membrane. This in turn defines a number of limitations on the operation of a conventional system, namely (i) extremely high levels of gas purity (>99.999%) specifically for electronic applications, cannot be directly obtained from the electrolyzer without requiring further purification [105], (ii) operation at low loads and at frequently changing loads reduces the life time of the membrane and further increases the potential for gas crossover [85] and (iii) production of hydrogen at high pressure requires a high differential pressure across the membrane [106]. To maintain the integrity of the membrane a thicker membrane is used in these circumstances resulting in a higher cell resistance and consequently lower efficiency. In this respect it is interesting to see if water electrolysis could be done in a fundamentally different way, perhaps mirroring the activation of water in photosynthesis which has two sets of coupled processes, i.e., a light reaction which results in oxygen evolution and a dark reaction which harnesses the proton gradient and electrons for organic activation.

Work by Cronin et al. [107−109] has demonstrated that a new route to water splitting is possible, and the limitations described above can be circumvented by the decoupling of the hydrogen and oxygen production via the introduction of a redox mediator, known as an *electron coupled proton buffer (ECPB)* into the cathode of the electrolyzer cell. This mediator effectively intercepts the electrons formed by water oxidation, being itself reduced, and the consequent increase in negative charge is balanced by the protons formed (Fig. 24.14A) which are associated with the reduced mediator. The hydrogen evolution reaction can then be carried out in a separate device (Fig. 24.14B) regenerating the oxidized ECPB ready for reuse.

The ability to act as an ECPB is determined by the position of the redox waves associated with the oxidation and reduction of the ECPB. To function as an ECPB the oxidations and reductions must occur at potentials between the oxygen and hydrogen evolving reactions. This allows the ECPB to "intercept" the electrons at a more positive potential than that required to combine with the protons to form hydrogen. This is illustrated in Fig. 24.15. The ECPB, in this case phosphomolybdic acid (solid line), demonstrates its electrochemical activity in the window between the oxidation of water and the reduction of protons (dashed line).

Cronin and coworkers have identified four different redox mediator types, which show great promise in decoupling hydrogen and oxygen production.

1. The polyoxometalate phosphomolybdic acid is used to decouple hydrogen and oxygen production resulting in two separate electrochemical steps [107].
2. The properties of the inorganic ECPB were extended to an organic system composed of potassium hydroquinone sulfonate [109].
3. By choosing the polyoxometalate silicotungstic acid, a highly asymmetric behavior was discovered wherein only a single electrochemical input was required [108]. This electrochemical step produced the reduced form of the silicotungstic acid; however, it was found that instead of a second electrochemical input to oxidize the acid and produce the hydrogen, this step could be successfully carried out by contact of the reduced ECPB with a suitable catalyst with no further electrical input (Fig. 24.16).

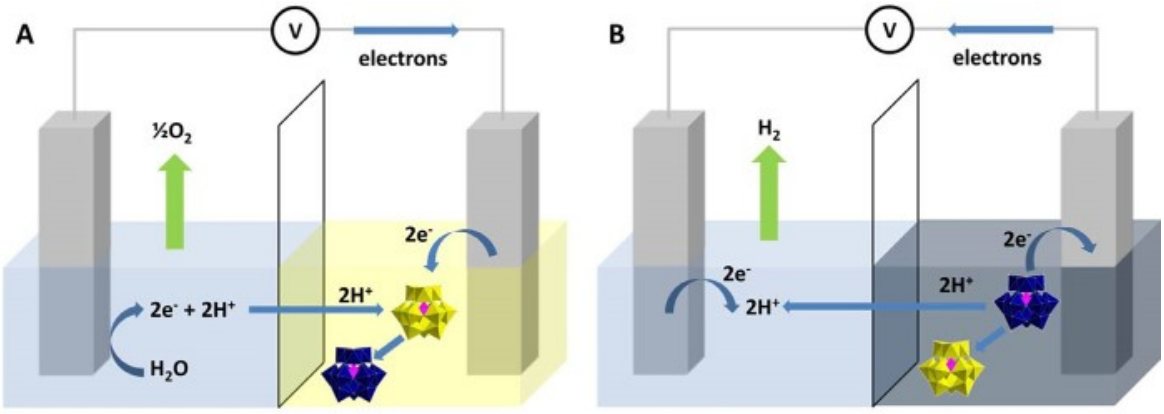

Figure 24.14 lectron coupled proton buffer (ECPB)-mediated oxygen and hydrogen generation. Reprinted by permission from M.D. Symes, L. Cronin, Decoupling hydrogen and oxygen evolution during electrolytic water splitting using an electron-coupled-proton buffer, Nat. Chem. (2013) Springer Nature.

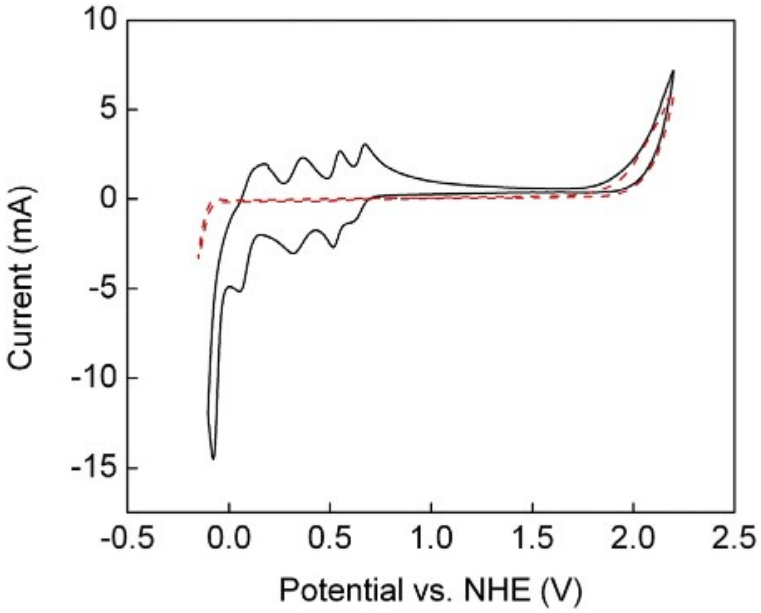

Figure 24.15 Comparison of ECPB reduction potentials with water electrolysis potentials. Reprinted by permission from M.D. Symes, L. Cronin Decoupling hydrogen and oxygen evolution during electrolytic water splitting using an electron-coupled-proton buffer, Nat. Chem. (2013) Springer Nature:

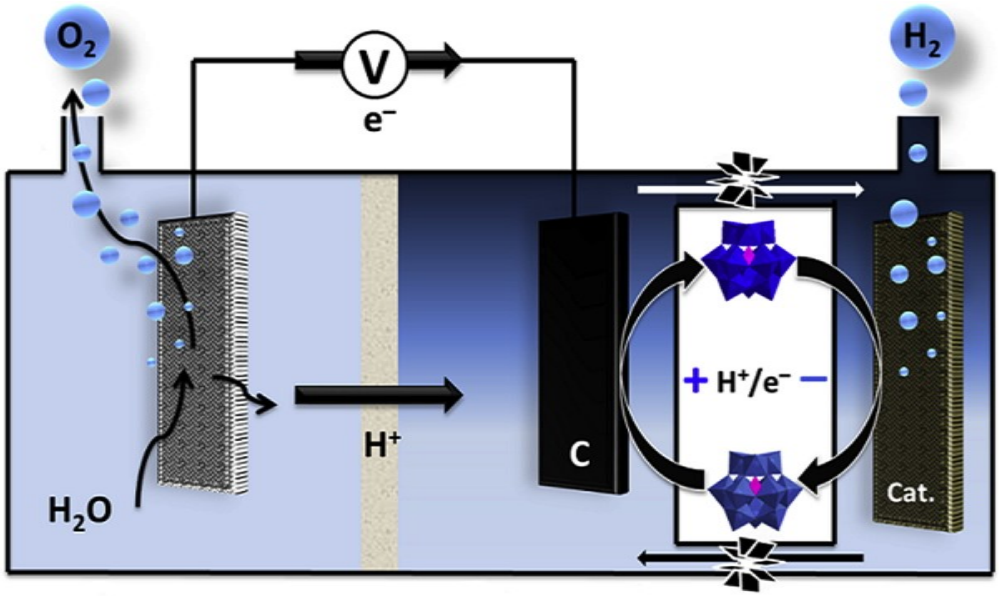

Figure 24.16 ECPB-mediated electrolysis using a single electrochemical input. From B. Rausch, M.D. Symes, G. Chisholm, L. Cronin, Science 345 (2014) 1326–1330. Reprinted with permission from AAAS.

4. The above redox mediators are limited to storing up to two electrons per molecule. Recent work has shown $Li_6[P_2W_{18}O_{62}]$ to be able to reversibly store up to 18 electrons [110].

By separating the production of hydrogen from oxygen, devices based on ECPBs have the potential to overcome the low load, high pressure/efficiency, and purity limitations of conventional electrolyzers [111].

Direct solar-to-hydrogen conversion in photoelectrochemical cells is a promising electrolysis technique for hydrogen generation. Recent research from Sun and coworkers showed the use of iron-based coordination complexes (ferrocenylmethyl) trimethylammonium chloride (FcNCl) to decouple the hydrogen evolution reaction (HER) and oxygen evolution reaction (OER) during water splitting in a neutral electrolyte (Fig. 24.17), ER is the FcNCl electrolyte. This system showed effective and durable operation (over 20 OER/HER cycles) when driven by photovoltaic cells [112].

Another promising technology is decoupling oxygen and hydrogen production with a solid-state redox mediator. The groups of Rothschild and Wang developed such systems independently, which rely on the REDOX processes of nickel (oxy)hydroxides (Fig. 24.18). Both studies reported excellent decoupling efficiencies and stabilities over multiple cycles. Rothschild's research demonstrated driving a decoupled water splitting process with solar energy input achieving a solar-to-hydrogen conversion efficiency of 7.5% [114].

Wang and Xia's group showcased another application. They developed a new type of battery (NiOOH—Zn based) which can alternately generate H_2 and electrical charge through replacing the OER couple by the anodic oxidation of zinc ($Zn \rightarrow ZnO_2^{2-}$) [113].

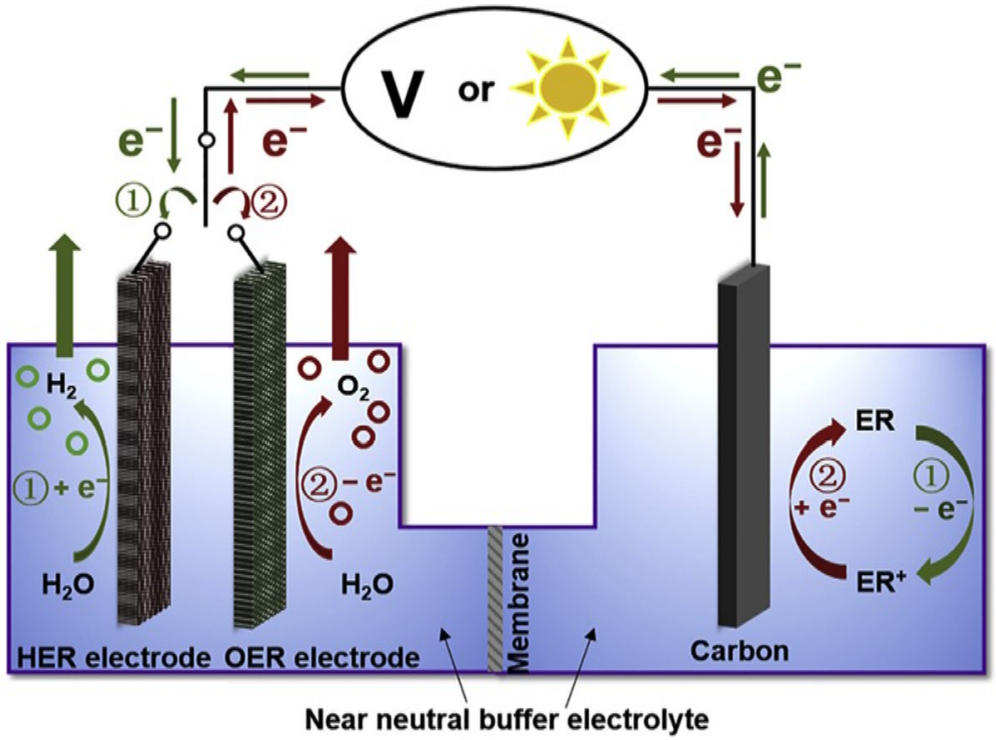

Figure 24.17 An electrolyzer for decoupled water splitting in near-neutral electrolyte. Reprinted from W. Li, N. Jiang, B. Hu, X. Liu, F. Song, G. Han et al., Electrolyser design for flexible decoupled water splitting and organic upgrading with electron reservoirs, Chem, 4 (2017) 637—649, Copyright, with permission from Elsevier.

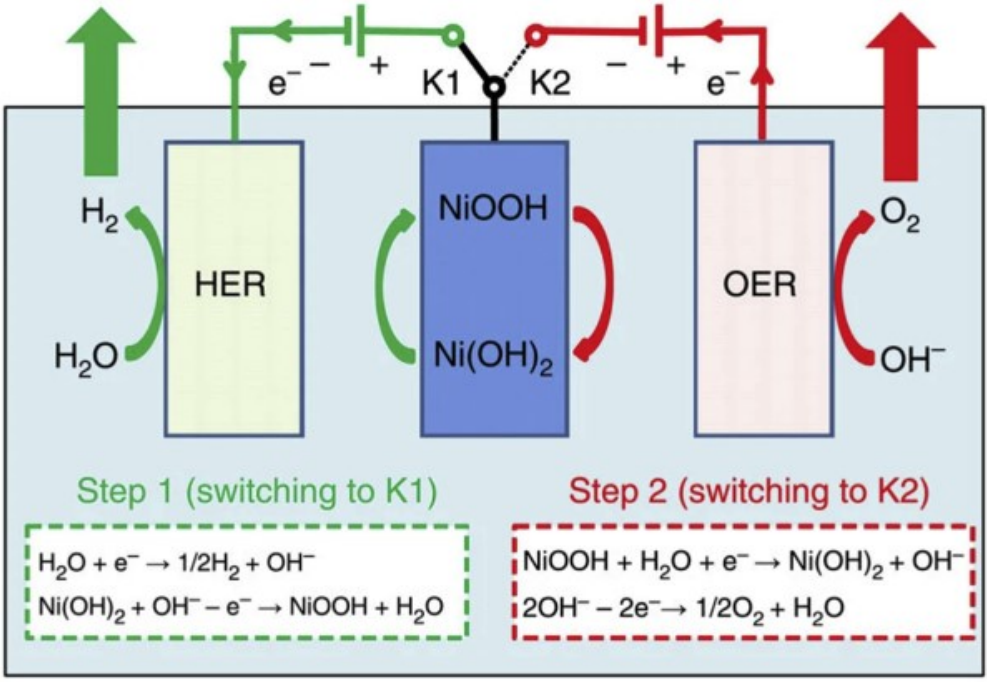

Figure 24.18 General diagram of decoupled water splitting using nickel (oxy)hydroxides as a solid-state redox mediator [113].
Reproduced under Creative Commons Attribution 4.0 International (CC BY 4.0).

6.2 *Flow battery/electrolyzer hybrids*

Redox flow batteries are a potential competitor technology to electrolysis as a route to economic and flexible energy storage and are discussed at length elsewhere in this volume. There is a promising technology which serves to exploit elements of both flow batteries and electrolyzers to produce hydrogen from water.

Amstutz et al. have recently developed a system based on indirect water electrolysis [115]. This system shares some commonalities with the ECPB concept described above in that the water splitting reactions occur in two distinct liquid circuits of the device. This allows the water oxidation reaction to address a limitation of the flow battery wherein the flow battery has a fixed capacity and once this is reached no further energy can be stored. In having an additional water oxidation capability, hydrogen can be produced as an adjunct to the electrochemical energy storage of the flow battery. The system described is a Ce—V flow battery (Fig. 24.19).

The electrochemical charging of the flow battery proceeds via the following reactions during charging (Scheme 24.6):

Once charging is complete or simultaneous to charging, the reduced V(II) species can be passed through a catalytic bed wherein it is oxidized to V(III) providing further V(III) for charging and producing hydrogen gas via the following overall reaction (Scheme 24.7):

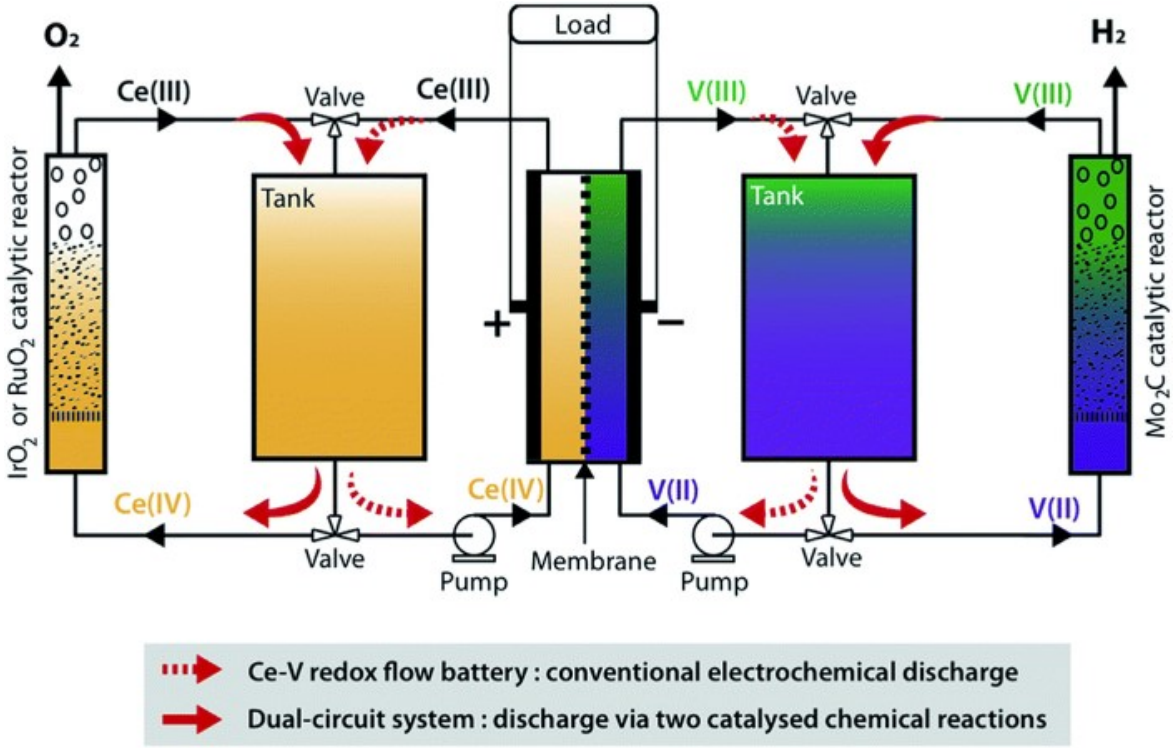

Figure 24.19 Ce−V dual-circuit flow battery.
Reproduced from Ref. V. Amstutz, K.E. Toghill, F. Powlesland, H. Vrubel, C. Comninellis, X. Hu, et al., Energy Environ. Sci. 7 (2014) 2350−2358 with permission from the Royal Society of Chemistry.

Cathode Reaction

$$V^{3+}_{(aq)} + e^- \longrightarrow V^{2+}_{(aq)}$$

Anode Reaction

$$Ce^{3+} \longrightarrow Ce^{4+} + e^-$$

Scheme 24.6 Ce−V flow battery reactions.

$$2H^+_{(aq)} + 2V^{2+}_{(aq)} \xrightarrow{Mo_2C} H_{2(g)} + 2V^{3+}_{(aq)}$$

Scheme 24.7 Hydrogen production from Ce−V flow battery.

As previously noted, the electrocatalyst most commonly used for hydrogen evolution in a conventional electrolyzer is platinum. The catalyst which is used in this system is molybdenum carbide (Mo_2C). It should also be noted that the production of hydrogen via the oxidation of V(II) does not require an additional electrochemical input to produce the hydrogen gas.

This concept has been further developed utilizing an all-vanadium system wherein hydrogen is produced from the oxidation of hydrogen sulfide [116]. It is not possible to

directly oxidize water in the all-vanadium system as the standard electrode potential for the VO_2^+/VO^{2+} redox couple is lower than that of water; hence, the need to provide another source of protons, in this case hydrogen sulfide. A similar dual circuit flow battery electrolyzer using hydrazine hydrate as the proton source has also been demonstrated [117,118].

6.3 Hydrogen from sea water

Generation of hydrogen from water requires a suitable water supply, free from contaminating ions which can corrode electrodes, poison membranes, or compete in electrochemical reactions. Fresh water can be a scarce resource in certain parts of the world, and this could be a limitation for the deployment of electrolyzers. Seawater is an effectively limitless resource; however, due to its ionic content it is not suitable for use in current electrolyzer technologies due to both chlorine formation competing favorably with oxygen formation at acidic pH and corrosion of electrolyzer components. Dai and coworkers [119] have addressed these twin issues by designing a corrosion-resistant electrode suitable for use in a sea water—based alkaline electrolyzer. This electrode is based on a layered nickel-iron hydroxide on top of nickel sulfide with a nickel foam as the core. The light-driven electrolysis rate (solar-to-hydrogen efficiency) was 11.9%, compared to 12.3% reported for a system utilizing pure water [120]. This solar-driven seawater-electrolzser was shown to be stable for 20 h without performance decay. The new method of electrolysis with seawater will open doors for availability of hydrogen fuel powered by renewable solar or wind energy.

7. Conclusion

The increase in renewable penetration in electricity generation and the increasing recognition that such penetration can only be managed via energy storage offers tremendous potential for the exploitation of established and nascent electrolysis processes in providing a solution to the energy storage dilemma. In addition, when one considers the slow, but steady emergence of the hydrogen-fueled vehicle market, the signs are extremely positive for a hydrogen economy and thus for the electrolysis industry required to support this.

References

[1] Global Overview, Paris, 2020.
[2] BP Statistical Review of World Energy, BP P.L.C., 2014.
[3] W.M. Haynes, D.R. Lide, CRC Handbook of Chemistry and Physics: A Ready-Reference Book of Chemical and Physical Data, CRC Press, 2011.
[4] Report of the Hydrogen Production Expert Panel: A Subcommittee of the Hydrogen & Fuel Cell Technical Advisory Committee, 2013.

[5] R. de Levie, J. Electroanal. Chem. 476 (1999) 92–93.
[6] H. Berg, Rev. Polarogr. 54 (2008) 99–103.
[7] J. Zhang, L. Zhang, H. Liu, A. Sun, R.S. Liu, Electrochemical Technologies for Energy Storage and Conversion, Wiley, 2012.
[8] W. Kreuter, Int. J. Hydrogen Energy 23 (1998) 661–666.
[9] D.H. Marie-Cecile Pera Hamid Gualous, C. Turpin, Electrochemical Components, Wiley, United Kingdom, 2013.
[10] R.R.K.W. Harrison, G.D. Martin, A. Hoskin, N.R.E. Laboratory, Hydrogen Production: Fundamentals and Case Study Summaries, 2010. Oak Ridge, TN, USA.
[11] S.Y. Gomez, D. Hotza, RSC Energy Environ. Ser. 25 (2020) 136–179.
[12] T.F.I. Smolinka, M.(F.I. Günther, J. (Fcbat) Garche, NOW-Studie 2011 (2010) 53.
[13] L. Bertuccioli, A. Chan, D. Hart, F. Lehner, B. Madden, E. Standen, Fuel Cells and Hydrogen Joint Undertaking - Development of Water Electrolysis in the European Union, 2014.
[14] A. Ursua, L.M. Gandia, P. Sanchis, Proc. IEEE 100 (2012) 410–426.
[15] S. Marini, P. Salvi, P. Nelli, R. Pesenti, M. Villa, M. Berrettoni, et al., Electrochim. Acta 82 (2012) 384–391.
[16] V. Schröder, B. Emonts, H. Janßen, H.-P. Schulze, Chem. Eng. Technol. 27 (2004) 847–851.
[17] H. Ito, T. Maeda, A. Nakano, H. Takenaka, Int. J. Hydrogen Energy 36 (2011) 10527–10540.
[18] M. Chandesris, V. Médeau, N. Guillet, S. Chelghoum, D. Thoby, F. Fouda-Onana, Int. J. Hydrogen Energy 40 (2015) 1353–1366.
[19] A. Goñi-Urtiaga, D. Presvytes, K. Scott, Int. J. Hydrogen Energy 37 (2012) 3358–3372.
[20] K.E. Ayers, C. Capuano, E.B. Anderson, ECS Trans 41 (2012) 15–22.
[21] M.H. Miles, M.A. Thomason, J. Electrochem. Soc. 123 (1976) 1459–1461.
[22] Z. Wei, J. Sun, Y. Li, A.K. Datye, Y. Wang, Chem. Soc. Rev. 41 (2012) 7994–8008.
[23] N. Coutard, N. Kaeffer, V. Artero, Chem. Commun. 52 (2016) 13728–13748.
[24] S. Kaufhold, L. Petermann, R. Staehle, S. Rau, Coord. Chem. Rev. 304–305 (2015) 73–87.
[25] D. Yang, Y. Chen, Z. Su, X. Zhang, W. Zhang, K. Srinivas, Coord. Chem. Rev. 428 (2021) 213619.
[26] W.-J. Jiang, T. Tang, Y. Zhang, J.-S. Hu, Acc. Chem. Res. 53 (2020) 1111–1123.
[27] Z. Lei, T. Wang, B. Zhao, W. Cai, Y. Liu, S. Jiao, et al., Adv. Energy Mater. 10 (2020) 2000478.
[28] J. Yu, Q. He, G. Yang, W. Zhou, Z. Shao, M. Ni, ACS Catal. 9 (2019) 9973–10011.
[29] E. Fabbri, T.J. Schmidt, ACS Catal. 8 (2018) 9765–9774.
[30] S. Anantharaj, S.R. Ede, K. Sakthikumar, K. Karthick, S. Mishra, S. Kundu, ACS Catal. 6 (2016) 8069–8097.
[31] G. Chisholm, P.J. Kitson, N.D. Kirkaldy, L.G. Bloor, L. Cronin, Energy Environ. Sci. 7 (2014) 3026–3032.
[32] L. Bi, S. Boulfrad, E. Traversa, Chem. Soc. Rev. 43 (2014) 8255–8270.
[33] M. Ni, M. Leung, D. Leung, Int. J. Hydrogen Energy 33 (2008) 2337–2354.
[34] N.Q. Minh, J. Am. Ceram. Soc. 76 (1993) 563–588.
[35] K.D. Kreuer, Annu. Rev. Mater. Res. 33 (2003) 333–359.
[36] M. Paria, Solid State Ionics 13 (1984) 285–292.
[37] H. Cavendish, Phil. Trans. 56 (1766) 141–184.
[38] J.L.C. Rowsell, O.M. Yaghi, Angew. Chem. Int. Ed. 44 (2005) 4670–4679.
[39] R. von Helmolt, U. Eberle, J. Power Sources 165 (2007) 833–843.

[40] DOE Technical Targets for Onboard Hydrogen Storage for Light-Duty Vehicles | Department of Energy. https://www.energy.gov/eere/fuelcells/doe-technical-targets-onboard-hydrogen-storage-light-duty-vehicles. Accessed December 14, 2020.
[41] A.R. Troiano, Trans ASM 52 (1960) 54–80.
[42] R.M. Vennett, G. Ansell, Trans ASM 60 (1967) 242–251.
[43] R.B. Benson, R.K. Dann, L.W. Roberts, Trans AIME 242 (1968) 2199–2205.
[44] T.P. Perng, C.J. Altstetter, Metall. Trans. A, Phys. Metall. Mater. Sci. 18 A (1987) 123–134.
[45] S. Lynch, Corrosion Rev. 30 (2012) 105–123.
[46] J. Zheng, X. Liu, P. Xu, P. Liu, Y. Zhao, J. Yang, Int. J. Hydrogen Energy 37 (2012) 1048–1057.
[47] H. Barthélémy, Int. J. Hydrogen Energy 37 (2012) 17364–17372.
[48] T.Q. Hua, R. Ahluwalia, J.K. Peng, M. Kromer, S. Lasher, K. McKenney, et al., Int. J. Hydrogen Energy 36 (2011) 3037–3049.
[49] D.J. Durbin, C. Malardier-Jugroot, Int. J. Hydrogen Energy 38 (2013) 14595–14617.
[50] S.W. Jorgensen, Curr. Opin. Solid State Mater. Sci. 15 (2011) 39–43.
[51] R.K. Ahluwalia, T.Q. Hua, J.K. Peng, S. Lasher, K. McKenney, J. Sinha, et al., Int. J. Hydrogen Energy 35 (2010) 4171–4184.
[52] S.M. Aceves, F. Espinosa-Loza, E. Ledesma-Orozco, T.O. Ross, A.H. Weisberg, T.C. Brunner, et al., Int. J. Hydrogen Energy 35 (2010) 1219–1226.
[53] N. Armaroli, V. Balzani, ChemSusChem 4 (2011) 21–36.
[54] E. Poirier, A. Dailly, Phys. Chem. Chem. Phys. (2012) 16544–16551.
[55] E. Poirier, A. Dailly, Langmuir 25 (2009) 12169–12176.
[56] A.F. Dalebrook, W. Gan, M. Grasemann, S. Moret, G. Laurenczy, Chem. Commun. 49 (2013) 8735–8751.
[57] M. Rzepka, P. Lamp, M.A. de la Casa-Lillo, J. Phys. Chem. B 102 (1998) 10894–10898.
[58] M. Jordá-Beneyto, F. Suárez-García, D. Lozano-Castelló, D. Cazorla-Amorós, a. Linares-Solano, Carbon N. Y. 45 (2007) 293–303.
[59] H.-L. Jiang, B. Liu, Y.-Q. Lan, K. Kuratani, T. Akita, H. Shioyama, et al., J. Am. Chem. Soc. 133 (2011) 11854–11857.
[60] S.H. Aboutalebi, S. Aminorroaya-Yamini, I. Nevirkovets, K. Konstantinov, H.K. Liu, Adv. Energy Mater. 2 (2012) 1439–1446.
[61] P.M. Budd, A. Butler, J. Selbie, K. Mahmood, N.B. McKeown, B. Ghanem, et al., Phys. Chem. Chem. Phys. 9 (2007) 1802–1808.
[62] C.D. Wood, B. Tan, A. Trewin, H. Niu, D. Bradshaw, M.J. Rosseinsky, et al., Chem. Mater. 19 (2007) 2034–2048.
[63] H. Furukawa, O.M. Yaghi, J. Am. Chem. Soc. 131 (2009) 8875–8883.
[64] Y. Li, R.T. Yang, J. Phys. Chem. B 110 (2006) 17175–17181.
[65] J. Dong, X. Wang, H. Xu, Q. Zhao, J. Li, Int. J. Hydrogen Energy 32 (2007) 4998–5004.
[66] U. Stoeck, S. Krause, V. Bon, I. Senkovska, S. Kaskel, Chem. Commun. 48 (2012) 10841.
[67] O.K. Farha, Ö. YazaydınA, I. Eryazici, C.D. Malliakas, B.G. Hauser, M.G. Kanatzidis, et al., Nat. Chem. 2 (2010) 944–948.
[68] H. Lee, J. Lee, D.Y. Kim, J. Park, Y.-T. Seo, H. Zeng, et al., Nature 434 (2005) 743–746.
[69] S. Dutta, J. Ind. Eng. Chem. 20 (2014) 1148–1156.
[70] L. Schlapbach, A. Züttel, Nature 414 (2001) 353–358.

[71] Handbook of Hydrogen Storage: New Materials for Future Energy Storage | Wiley. https://www.wiley.com/en-gb/Handbook+of+Hydrogen+Storage%3A+New+Materials+for+Future+Energy+Storage-p-9783527322732. Accessed December 14, 2020.
[72] J. Mao, D. Gregory, Energies 8 (2015) 430–453.
[73] P. Chen, Z. Xiong, J. Luo, J. Lin, K.L. Tan, Nature 420 (2002) 302–304.
[74] H. Jindal, A.S. Oberoi, I.S. Sandhu, M. Chitkara, Potential porous mediums for electrochemical hydrogen storage: state of art and comparative study, in: Mater. Today Proc., Elsevier Ltd, 2020, pp. 1888–1898.
[75] F. Zhang, P. Zhao, M. Niu, J. Maddy, Int. J. Hydrogen Energy 41 (2016) 14535–14552.
[76] L. George, S.K. Saxena, Int. J. Hydrogen Energy 35 (2010) 5454–5470.
[77] P. Jena, J. Phys. Chem. Lett. 2 (2011) 206–211.
[78] Y. Kojima, Y. Kawai, J. Alloys Compd. 395 (2005) 236–239.
[79] M.B. Ley, L.H. Jepsen, Y.S. Lee, Y.W. Cho, J.M. Bellosta Von Colbe, M. Dornheim, et al., Mater. Today 17 (2014) 122–128.
[80] I. MacLeay, K. Harris, A. Annut, C. Authors, Digest of United Kingdom Energy Statistics, DUKES), 2013, p. 2013.
[81] M. Ilbas, a.P. Crayford, I. Yilmaz, P.J. Bowen, N. Syred, Int. J. Hydrogen Energy 31 (2006) 1768–1779.
[82] Gas Quality. http://www2.nationalgrid.com/uk/industry-information/gas-transmission-system-operations/gas-quality/. Accessed April 3, 2015.
[83] K. Yaccato, R. Carhart, A. Hagemeyer, A. Lesik, P. Strasser, A.F. Volpe, et al., Appl. Catal. Gen. 296 (2005) 30–48.
[84] W. Wang, J. Gong, Front. Chem. Eng. China 5 (2011) 2–10.
[85] S.A. Grigoriev, V.I. Porembskiy, S. V Korobtsev, V.N. Fateev, F. Aupretre, P. Millet, Int. J. Hydrogen Energy 36 (2011) 2721–2728.
[86] G.S. Burkhanov, N.B. Gorina, N.B. Kolchugina, N.R. Roshan, D.I. Slovetsky, E.M. Chistov, Platin. Met. Rev. 55 (2011) 3–12.
[87] DeOxo. https://catalysts.basf.com/literature-library/adsorbents/adsorbents-for-deoxo. Accessed December 14, 2020.
[88] M. Succi, S. Pirola, S. Ruffenach, O. Briot, Cryst. Res. Technol. 46 (2011) 809–812.
[89] M. Inaba, T. Kinumoto, M. Kiriake, R. Umebayashi, A. Tasaka, Z. Ogumi, Electrochim. Acta 51 (2006) 5746–5753.
[90] A. Szyszka, Int. J. Hydrogen Energy 23 (1998) 849–860.
[91] Hydrogen: A Renewable Energy Perspective. https://www.irena.org/publications/2019/Sep/Hydrogen-A-renewable-energy-perspective. Accessed December 14, 2020.
[92] Hybridge - A Project of Amprion and Open Grid Europe. https://www.hybridge.net/index-2.html. Accessed December 14, 2020.
[93] About – REFHYNE. https://refhyne.eu/about/. Accessed December 14, 2020.
[94] ElementEINS - ElementEins. https://www.element-eins.eu/. Accessed December 14, 2020.
[95] Energiepark Bad Lauchstädt. https://www.dbi-gruppe.de/energieparkBL.html. Accessed December 14, 2020.
[96] Steel Manufacturing - thyssenkrupp. https://www.thyssenkrupp-steel.com/en/. Accessed December 14, 2020.
[97] Power to Gas. https://www.energiedienst.de/produktion/wasserstoff/power-to-gas/. Accessed December 14, 2020.
[98] HydroHub-Fenne to become a Real-World Laboratory: STEAG GmbH. https://www.steag.com/en/press-release/19-07-2019-19-07-2019-hydrohub-fenne-to-become-a-real-world-laboratory-1. Accessed December 14, 2020.

[99] Fuel Cell. Bull. 2019 (2019) 14−15.
[100] Press Release Groundbreaking Agreement for Energy Revolution Signed-Green Light for Lusatia Reference Power Plant, 2019.
[101] reportGRHYD Report. https://en.calameo.com/read/0064495685b3772672648?page=1. Accessed January 18, 2021.
[102] Horizon Power Denham Hydrogen Demonstration. https://arena.gov.au/projects/horizon-power-denham-hydrogen-demonstration/.Accessed January 5, 2021.
[103] H2@Scale: Enabling Affordable, Reliable, Clean, And Secure Energy Across Sectors. https://www.energy.gov/sites/prod/files/2020/09/f79/h2-at-scale-crada-projects-2020.pdf. Accessed January 18, 2021.
[104] The world's largest-class hydrogen production, Fukushima Hydrogen Energy Research Field (FH2R) now is completed at Namie town in Fukushima. https://www.toshiba-energy.com/en/info/info2020_0307.htm. Accessed January 6, 2021.
[105] Bright ideas - Delivering Smarter LED Manufacturing Through Innovative Gas Technology. http://www.linde-gas.com/internet.global.lindegas.global/en/images/Linde_in_LED_brochure_WEB_1.117_39138.pdf Accessed April 30, 2015.
[106] M. Schalenbach, M. Carmo, D.L. Fritz, J. Mergel, D. Stolten, Int. J. Hydrogen Energy 38 (2013) 14921−14933.
[107] M.D. Symes, L. Cronin, Nat. Chem. 5 (2013) 403−409.
[108] B. Rausch, M.D. Symes, G. Chisholm, L. Cronin, Science 345 (2014) 1326−1330.
[109] B. Rausch, M.D. Symes, L. Cronin, J. Am. Chem. Soc. 135 (2013) 13656−13659.
[110] J.-J. Chen, M.D. Symes, L. Cronin, Nat. Chem. 10 (2018) 1042−1047.
[111] P.J. McHugh, A.D. Stergiou, M.D. Symes, Adv. Energy Mater. 10 (2020) 2002453.
[112] W. Li, N. Jiang, B. Hu, X. Liu, F. Song, G. Han, et al., Inside Chem. 4 (2018) 637−649.
[113] L. Chen, X. Dong, Y. Wang, Y. Xia, Nat. Commun. 7 (2016) 11741.
[114] A. Landman, H. Dotan, G.E. Shter, M. Wullenkord, A. Houaijia, A. Maljusch, et al., Nat. Mater. 16 (2017) 646−651.
[115] V. Amstutz, K.E. Toghill, F. Powlesland, H. Vrubel, C. Comninellis, X. Hu, et al., Energy Environ. Sci. 7 (2014) 2350−2358.
[116] P. Peljo, H. Vrubel, V. Amstutz, J. Pandard, J. Morgado, A. Santasalo-Aarnio, et al., Green Chem. 18 (2016) 1785−1797.
[117] D. Frey, J. Kim, Y. Dvorkin, M.A. Modestino, Cell Rep. Phys. Sci. 1 (2020) 100226.
[118] J. Piwek, C.R. Dennison, E. Frackowiak, H. Girault, A. Battistel, J. Power Sources 439 (2019) 227075.
[119] Y. Kuang, M.J. Kenney, Y. Meng, W.H. Hung, Y. Liu, J.E. Huang, et al., Proc. Natl. Acad. Sci. U.S.A. 116 (2019) 6624−6629.
[120] J. Luo, J.H. Im, M.T. Mayer, M. Schreier, M.K. Nazeeruddin, N.G. Park, et al., Science 345 (2014) 1593−1596.